A43F-0221

Preliminary results from the retrieval and assimilation of GPS radio occultation refractivity observations during tropical storm development

J.S. Haase[1], B. J. Murphy[2], X.-M. Chen[3], S.-H. Chen[3], P. Muradyan[2], F. Nievinski[4], K.M. Larson[4], J.L. Garrison[2], K.-N. Wang[2], S.-Y. Chen[5]

1. Scripps Institution of Oceanography, UCSD, La Jolla, CA 92093-0225 (jhaase@ucsd.edu) 2. Purdue University, West Lafayette, IN 47907 3. Dept of Land, Air & Water Resources, University of California, Davis, CA, 95616-8627 4. Aerospace Engineering Sciences, University of Colorado, Boulder, CO, 80309 5. University Corporation for Atmospheric Research, Boulder, CO, 80301

INTRODUCTION

For the first time, dense airborne GPS radio occultation (ARO) observations have been collected near developing cyclones, with concurrent dense sampling by dropsondes. in the 2010 PRE-Depression Investigation of Cloud systems in the Tropics (PREDICT) experiment, a large ARO dataset was acquired from twenty-six research flights and refractivity profiles have been derived from the GISMOS geodetic GPS receiver data. The airborne RO profiles consistently agree within ~2% of refractivity profiles calculated from the European Center for Medium-range Weather Forecasting (ECMWF) Interim Reanalysis (ERA-Interim) and dropsonde data. Changes in refractivity obtained from ARO data over the five days leading to the genesis of the tropical storm that would later develop into hurricane Karl are consistent with moistening in the vicinity of the storm center. The algorithm to assimilate airborne GPS observations has been implemented in the Three-Dimensional Variational (3DVAR) Data Assimilation (DA) system of the Weather Research and Forecasting (WRF) model. Preliminary experiments show a positive impact from the assimilation of both dropsondes and airborne GPS observations on Karl simulations, with improvements in refractivity and moisture fields above ~4 km. GPS signals from the GISMOS 10 MHz recording system have been analyzed with a more robust open loop tracking method and are shown to track ~2km deeper into the troposphere than the conventional receivers. These profiles will be used to improve the data assimilation at lower levels.

OBJECTIVES

To determine the ability of the airborne GPS radio occultation technique to resolve moisture variabilty in the region of a developing tropical storm.

To quantify the accuracy of refractivity profiles retrieved from airborne GPS radio occultation data by comparison to profiles derived from co-located dropsonde data and numerical weather prediction models.

To test the assimilation of airborne GPS radio occultation refractivity profiles into a numerical weather model during the development of a tropical system, and quantify the improvements in the model forecast accuracy.

THE PRE-DEPRESSION INVESTIGATION OF CLOUD SYSTEMS IN THE TROPICS CAMPAIGN (PREDICT)

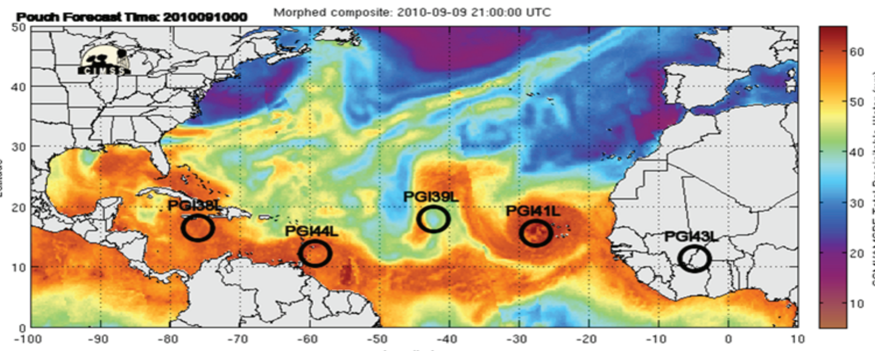

Most Atlantic hurricanes form in cloud systems associated with African Easterly Waves, troughs of low pressure which move off the African continent and across the Atlantic (Landsea 1993). In this image from 1 September 2010, areas of circulation co-moving with waves are labeled and tracked. These regions are isolated areas where convection can increase moisture leading to an environment in which a hurricane may form. The PRE-Depression Investigation of Cloud systems in the Tropics (PREDICT) experiment specifically studied the development phase of tropical cyclones. Measurements are centered about the axes of the African Easterly Waves. The figure above shows total precipitable water in the atmosphere around these regions based on satellite imagery and are provided by the Cooperative Institute for Meteorological Satellite Studies.

RADIO OCCULTATION GEOMETRIC RAY PATH

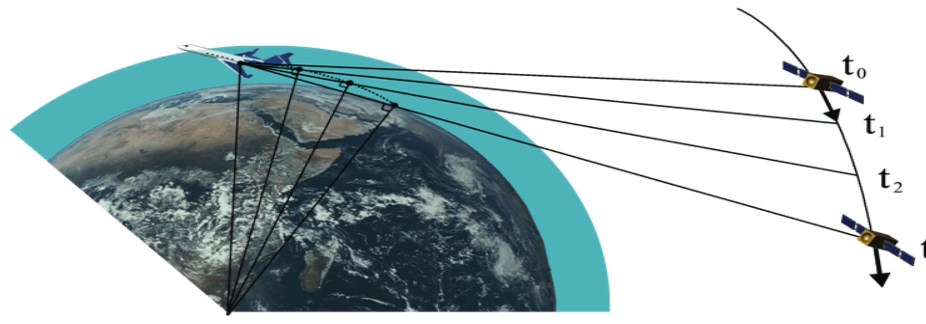

Illustration of GPS signal ray paths through the atmosphere from an occulting satellite setting below the horizon, and the tangent points of the ray paths, for the airborne GNSS Instrument System for Multistatic and Occultation Sensing (GISMOS) (Garrison et al., 2007). The line of sight to the GPS satellite initially has a positive elevation with respect to the horizon, then a negative elevation angle below the horizon, until it sets. When the ray is refracted in the atmosphere, under the approximation of spherical symmetry, the path can be defined by a bending angle, and is observed through the excess Doppler shift of the GPS signal carrier phase. The bending angle can be related to refractivity using geometric optics (Kursinski et al., 2000; Healy et al., 2002; Xie et al., 2008).

ACKNOWLEDGEMENTS

This work was funded by the following grants: HIAPER UCAR Subcontract S05-39696, NSF grant SGER-0802887, NSF grant AGS 1015904. Partial support for BM was provided by the Ross Fellowship. PM was supported by the Schlumberger Faculty for the Future Fellowship. UA was supported by a grant from the Republic of Turkey Ministry of National Education.
We would also like to thank the following:
A. Johnson assisted with the GISMOS data collection and preliminary analysis during the PREDICT campaign; S.-C. Chen and C.-Y. Huang at National Central University in Taiwan assisted with the data assimilation; J. Jensen, J. Meitin, A. Cooper, A. Schanot, R. Sherman, and the NCAR-EOL and NCAR-RAF staff for their logistical support during PREDICT; PREDICT PI's M. Montgomery and C. Davis; M. Bell, D. Raymond, and C. Lopez who assisted with GISMOS operation; J. Dunion, J. Cordeira, K. Griffin and the PREDICT/NASA/NOAA forecast teams.
Data products: Co-operative Institute for Meteorological Satellite Studies, European Center for Medium-range Weather Forecasts and the National Hurricane Center, NCAR EOL and NASA ESDIS dropsonde data sets, Z. Wang for providing hourly pouch tracks, F. Xie for his help with ECMWF data.

RESEARCH MISSION RF18 INTO DEVELOPING CYCLONE KARL

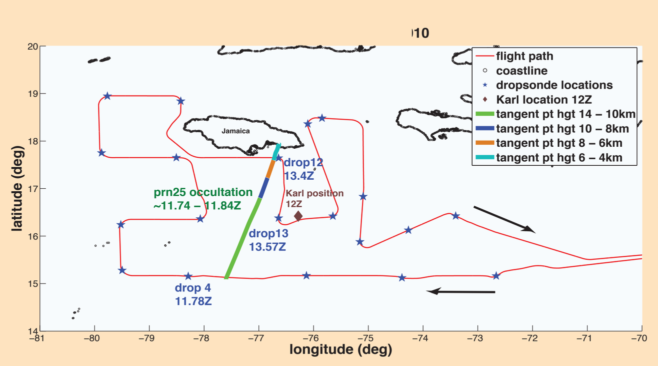

PREDICT RF18 13 September 2010

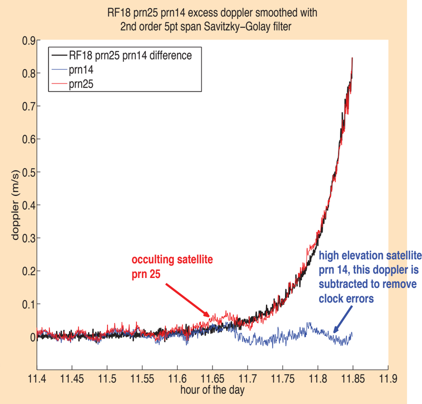

Excess doppler

Research flight 18 (13 September 2010, T-1 days) (above left) This flight targeted the pre-Karl system one day prior to genesis. The flight track and dropsonde locations (stars) are shown. The locations of the tangent points for the setting satellite prn25 occultation are shown with different colors indicating the tangent point heights. The location of the circulation center (Dunkerton et al. 2009) is shown with the diamond.
Excess Doppler (above right): The excess Doppler shift of the GPS carrier phase increases with time as the satellite sets and the refractive bending angle increases. The Doppler shift from a high elevation satellite, prn14, is subtracted from the prn25 Doppler.

RF18 prn25 minus prn14

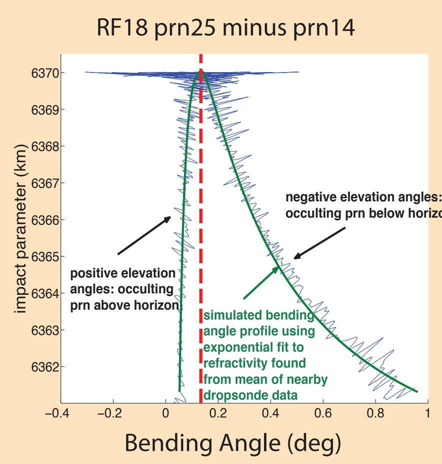

Bending Angle (deg)

RF18 prn25 refractivity retrieval

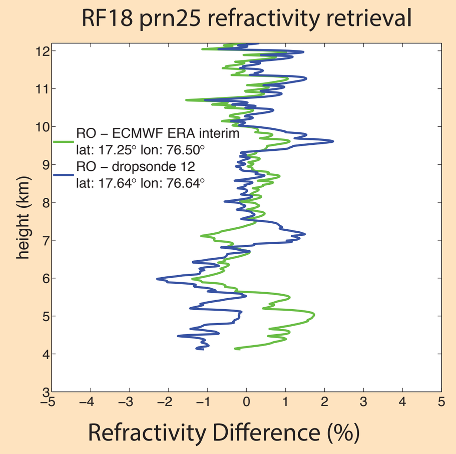

Refractivity Difference (%)

Bending angle: The refractive bending angle (blue) is retrieved from the excess Doppler and compared with a simulated profile (green) from ERA-Interim.

Refractivity : The profile retrieved from the prn25 occultation is compared with profiles calculated using a co-located dropsonde and the ERA-Interim model.

Open-loop tracking (right): The geodetic quality phase lock loop (PLL) receivers utilize a feedback tracking algorithm which will lose lock on a signal in the lower troposphere due to rapid phase fluctuations, for example, caused by sharply changing refractivity gradients. A GPS recorder was also used to directly sample the down-converted GPS RF signals at 10 MHz for post-processing with a software receiver using an open loop tracking algorithm. This makes it possible to track deeper into the troposphere (Acikoz, 2011; Muradyan et al., 2012;). In the plot at right, the refractivity retrieval for RF18 prn25 is extended ~2 km deeper than the retrieval using the PLL data.

RF18 prn25 open loop retrieval

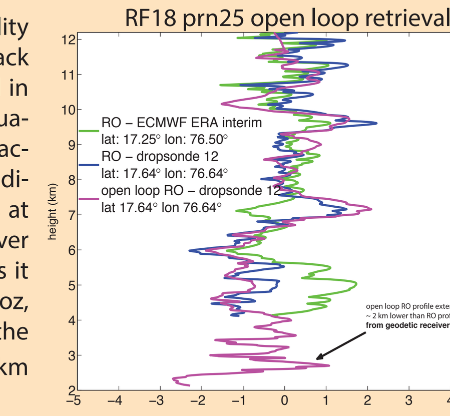

Refractivity Difference (%)

ASSESSING ARO DATA QUALITY: COMPARISONS TO DROPSONDES AND THE ECMWF MODEL

We use 21 profiles throughout the PREDICT campaign to assess the overall agreement of the ARO refractivity data with refractivity profiles derived from dropsondes and from the ERA-Interim model. Refractivity is calculated using:

$$N \cong 77.6\frac{P}{T} + 3.73 \times 10^5 \frac{e}{T^2}$$

where pressure, *P*, and water vapor pressure, *e*, are in hPa and *T* is in kelvin. The geometric height is found from geopotential height, accounting for variations in gravity and the geoid height above the WGS-84 ellipsoid.

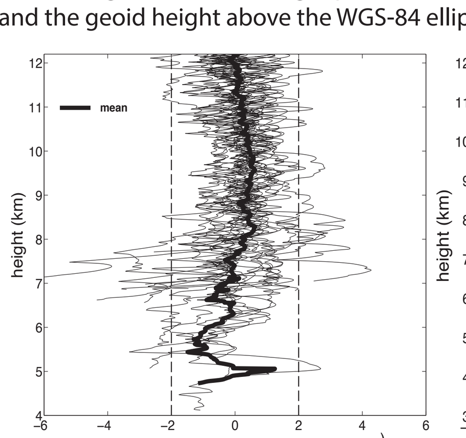

RO - dropsonde refractivity difference (%)

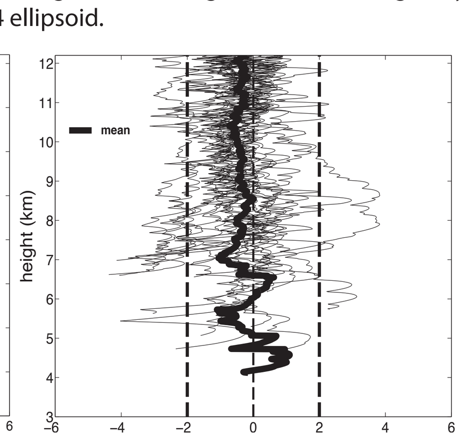

RO - ECMWF refractivity difference (%)

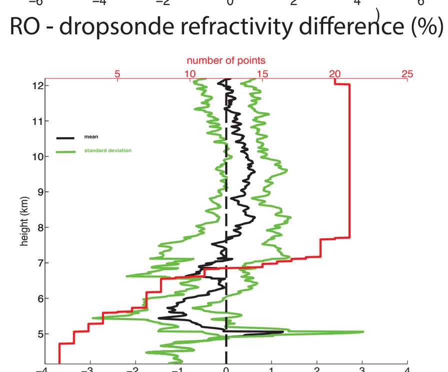

RO - dropsonde refractivity difference (%)

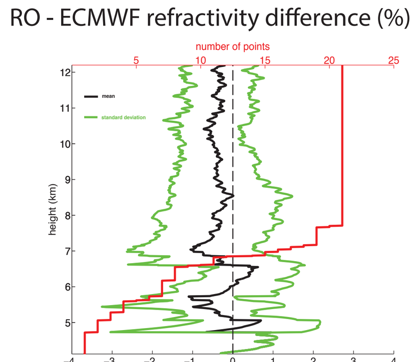

RO - ECMWF refractivity difference (%)

The average spatial separation between the dropsonde and RO occultation point is 118 km and the average separation in time is 1.4 hours. The RO – dropsonde differences are generally less than ~ 2 %.

The ECMWF ERA interim reanalysis is interpolated to 0.75 degrees in latitude and longitude. The mean difference for both RO – dropsonde and RO – ECMWF is less than 1 %.

EVOLUTION OF HURRICANE KARL

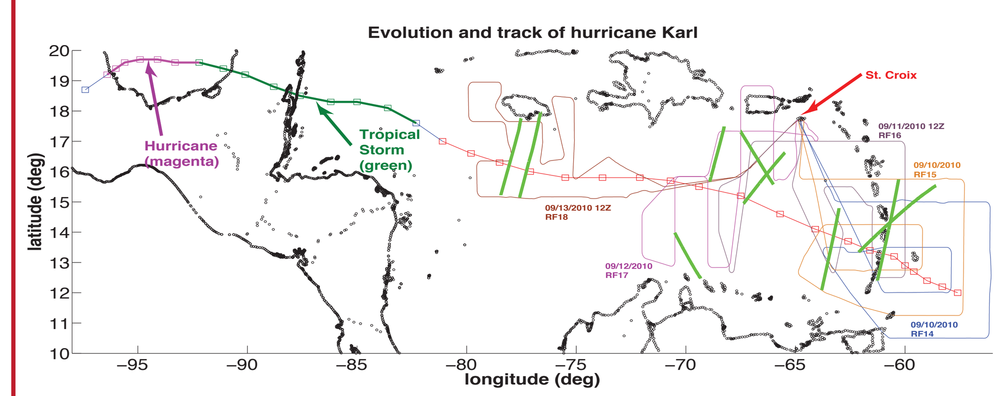

The development of Karl was studied extensively during PREDICT with six research flights into the system over five days, from 10 - 14 September 2010. Genesis occurred on 14 September when Karl became a tropical depression (T 0). It became a tropical storm later that day, was upgraded to a hurricane on 16 September, and reached its maximum intensity of Category 3 on 18 September (Stewart, 2011). It became the strongest hurricane to be recorded in the Bay of Campeche. Airborne GPS radio occultation refractivity profiles are presented in this study from five research flights, RF14 – RF18. Flight tracks are shown in the figure above. The tangent point drift paths for GPS satellite occultations recorded by GISMOS geodetic receivers are highlighted in green.

MOISTURE VARIABILITY AS SHOWN BY REFRACTIVITY IN DEVELOPING TROPICAL STORM KARL

Changes in refractivity relative to the 4-day mean serve as a proxy for moisture evolution as Karl transitions from a tropical disturbance to tropical depression and then to a tropical storm from 9-14 September.

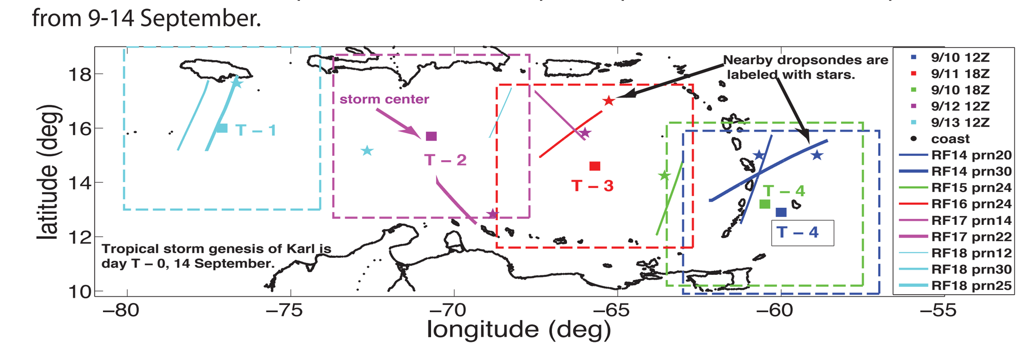

Locations of a subset of setting occultations for research flights RF14 – RF18, using geodetic receiver data. The tangent point paths of the occultations are shown for each flight. Stars give the location of dropsonde deployments nearest the occultation tangent points. The dropsonde and RO profiles closest to the center (squares) will be used to illustrate moisture evolution.

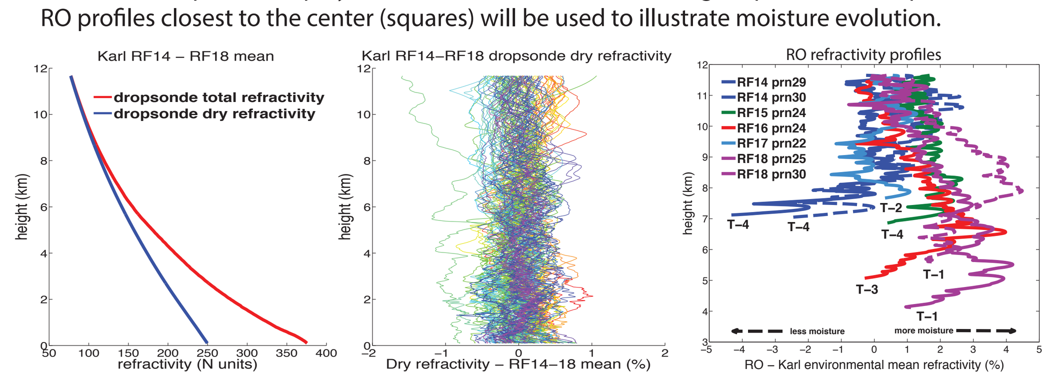

The dry refractivity, N_dry=77.6*(P/T), varies little over the four days (**above center**) where the dry refractivity calculated from each dropsonde is compared to the mean of all drops over RF14 - RF18. The refractivity variation below ~9km can be attributed mostly to moisture (**above left**), the approximate height where the mean total refractivity begins to deviate from the mean dry refractivity.
The RO refractivity profiles are consistent with a general moistening in the vicinity of the developing tropical storm (**above right**). The refractivity profile for each occultation is shown relative to the Karl environmental mean refractivity. The environmental mean was calculated from 105 drops over RF14-18. Later RO observations closer to genesis (genesis = T - 0) have significantly greater refractivity (> ~2%) in the height range from 6-8 km. The closest RO profiles to the storm center are from RF14 (T-4), RF16 (T-3) and RF18 (T-1).

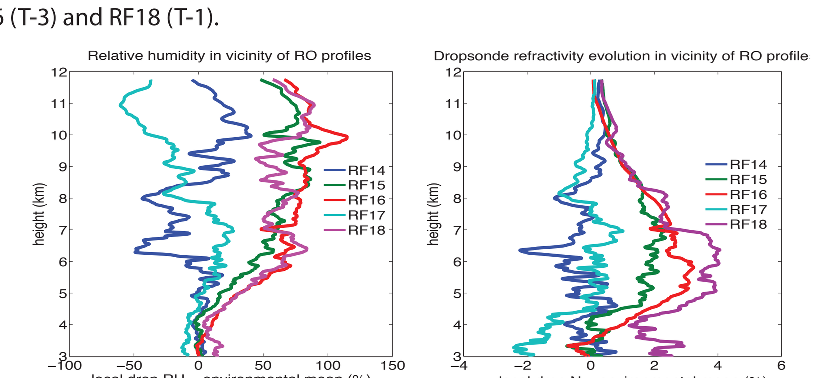

Averages from four dropsondes in the vicinity of occultations were calculated from each flight RF14 -RF18. The variation of relative humidity (left) and refractivity (right) from the 5 day environmental mean of 105 dropsondes is shown above.

* The most significant dropsonde moisture variations are in the 5-9 km height range that is well sampled by RO.

* Variations in refractivity over RF14-RF18 are consistent between dropsondes and RO.

* Dropsonde and RO refractivity profiles are consistent with moistening near the tropical cyclone

REFERENCES

Acikoz, U., 2011: Open-loop tracking of rising GPS radio occultation signals. MS Thesis, Dep. of Aeronautics and Astronautics Eng., Purdue University, West Lafayette, IN, US.
Chen, S.-H., and W.-Y. Sun, 2002: A one-dimensional time dependent cloud model. J. Meteorol. Soc. Jpn., 80, 99–118.
Chen, S.-Y., C.-Y. Huang, Y.-H. Kuo, Y.-R. Guo, and S. Sokolovskiy, 2009: Assimilation of GPS Refractivity from FORMOSAT-3/COSMIC Using a Nonlocal Operator with WRF 3DVAR and Its Impact on the Prediction of a Typhoon Event. Terr. Atmos. Ocean. Sci., 20, 133-154.
Chou, M.-D. and M. J. Suarez, 1999: A solar radiation parameterization for atmospheric studies. NASA Tech. Memo. 104606, 15, 40 pp.
Chou, M.-D., M. J. Suarez, X.-Z. Liang, and M. M.-H. Yan, 2001: A thermal infrared radiation parameterization for Atmospheric Studies. NASA Tech. Memo., 104606, 19, 102 pp.
Dunkerton, T. J., M.T. Montgomery, Z. Wang, Z., 2009: Tropical cyclogenesis in a tropical wave critical layer: easterly waves, Atmos. Chem. Phys., 9, 5587-5646.
Garrison, J. L., M. Walker, J. S. Haase, T. Lulich, F. Xie, B. D. Ventre, M. H. Boehme, B. Wilmhoff, and S. J. Katzberg, 2007: Development and Testing of the GISMOS Instrument, paper presented at IEEE International Geoscience and Remote Sensing Symposium, Barcelona, Spain, 23-27 July 2007.
Healy, S. B., Haase, J.S., and Lesne, O., 2002: Abel transform inversion of radio occultation measurements made with a receiver inside the Earth's atmosphere. Annales Geophysicae, 20, 1253-1256.
Hong, S.-Y. and H.-L. Pan, 1996: Nonlocal boundary layer vertical diffusion in a medium-range forecast model. Mon. Wea. Rev., 124, 2322-2339.
Kain, J. S., 2004: The Kain-Fritsch convective parameterization: An update. J. Appl. Meteor., 43, 170-181.
Kursinski, E. R., Hajj, G. A., Leroy, S. S., and Herrman, B., 2000: The GPS Radio Occultation Technique. TAO, 11, 1, 53-114.
Landsea, C. W., 1993: A climatology of intense (or major) Atlantic hurricanes. Monthly Weather Review, 121(6), 1703-1713.
Mlawer, E. J., S. J. Taubman, P. D. Brown, M. J. Iacono, and S. A. Clough, 1997: Radiative transfer for inhomogeneous atmospheres: RRTM, a validated correlated-k model for the long-wave. J. Geo. Res., 102, 16,663-16,682.
Muradyan, P., Haase, J. S., Acikoz, U., Garrison, J. L., Xie, F. , and Lulich, T. D., 2012: Profiling the atmosphere with the airborne GPS radio occultation technique using open-loop tracking, J. Geophys. Res, submitted.
Parrish, D.F. and J.C. Derber, 1992: The National Meteorological Center's Spectral Statistical-Interpolation Analysis System. Mon. Wea. Rev., AMS, 120, 1747-1763.
Smith, E. K. and Stanley Weintraub, 1953: The Constants in the Equation for Atmospheric Refractive Index at Radio Frequencies. Proceedings of the I.R.E, August, 1035-1037.
Stewart, S.R., 2011: Tropical Cyclone Report, Hurricane Karl. National Hurricane Center.

PRELIMINARY ASSIMILATION INTO THE WEATHER RESEARCH AND FORECASTING (WRF) MODEL

WRF MODEL CONFIGURATION

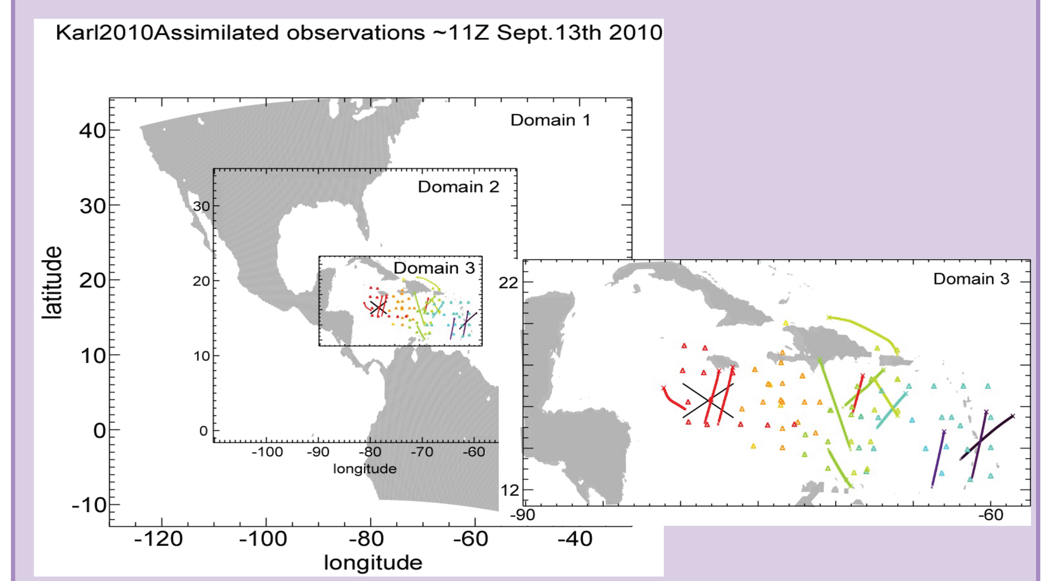

Three-way nested simulation domains (27 km, 9 km, and 3km grids) and locations of all assimilated observations during the data cycling period. Colors: 1200 UTC September 10th in violet to 1200 UTC September 13th in red. The large black cross indicates the position of the Tropical Low at 1800 UTC September 13th as reported by the National Hurricane Center (Stewart 2011).

Model configuration:
- Purdue microphysics scheme (Chen and Sun, 2002)
- YonSei University (YSU) planetary boundary layer scheme (Hong et al., 1996)
- Kain-Fritsch (KF) cumulus parameterization (Kain 2004),
- Rapid Radiative Transfer Model longwave radiation parameterization (Mlawer et al. 1997)
- Goddard shortwave radiation parameterization (Chou and Suarez 1999; Chou et al. 2001).
- A time step of 120 seconds is used for domain 1.
- Initial and boundary conditions are the NCEP FNL (Final) Operational Global Analysis

DATA ASSIMILATION EXPERIMENTS

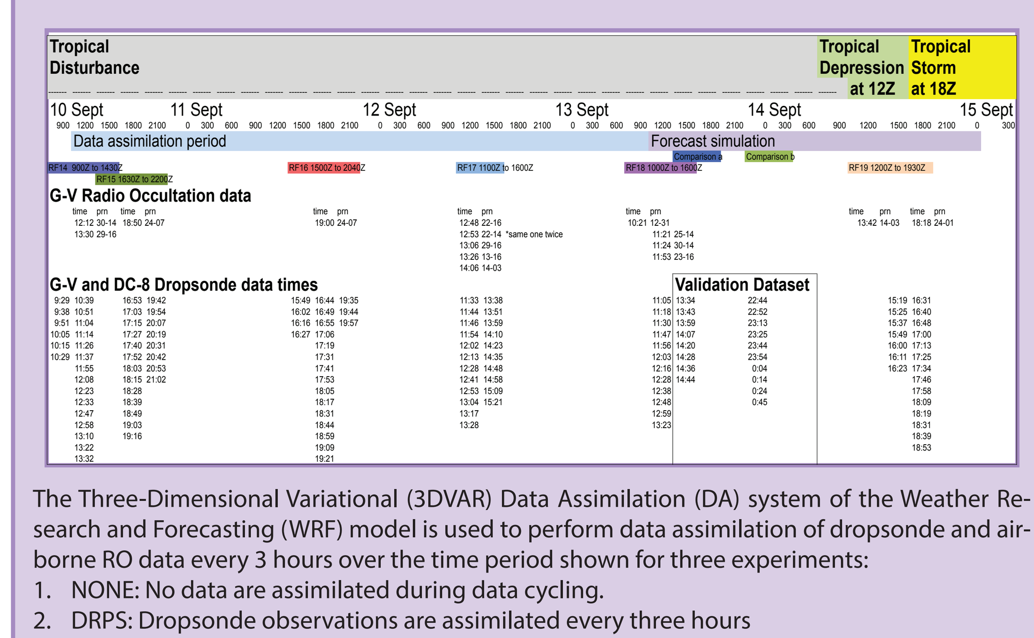

The Three-Dimensional Variational (3DVAR) Data Assimilation (DA) system of the Weather Research and Forecasting (WRF) model is used to perform data assimilation of dropsonde and airborne RO data every 3 hours over the time period shown for three experiments:
1. NONE: No data are assimilated during data cycling.
2. DRPS: Dropsonde observations are assimilated every three hours
3. DRPS+GPS: Airborne GPS refractivity data are added to the DRPS experiment, providing additional information on the refractivity of the air column, mainly above 5km.

* The vertical profiles are thinned to one observation per model level to avoid over-weighting and correlation of observational errors.
* Background error covariance was calculated with the NMC method (Parrish and Derber, 1992) using 12 and 24-hours model forecast differences from the WRF model for September 2010.
* ARO observation errors were estimated to be 2% and constant over height from 0 to 14 km based on the comparison completed at left.
* A non-local operator for integrated excess phase along the GPS ray path (Chen et al., 2009) has been modified from the space-borne geometry to account for the truncation of the observations at the aircraft flight level and to account for the horizontal drift of the tangent points.
* Three external iterations are performed at each data assimilation cycle to assure balance before propagating forward.

DROPSONDE ONLY ASSIMILATION USING WRFDA

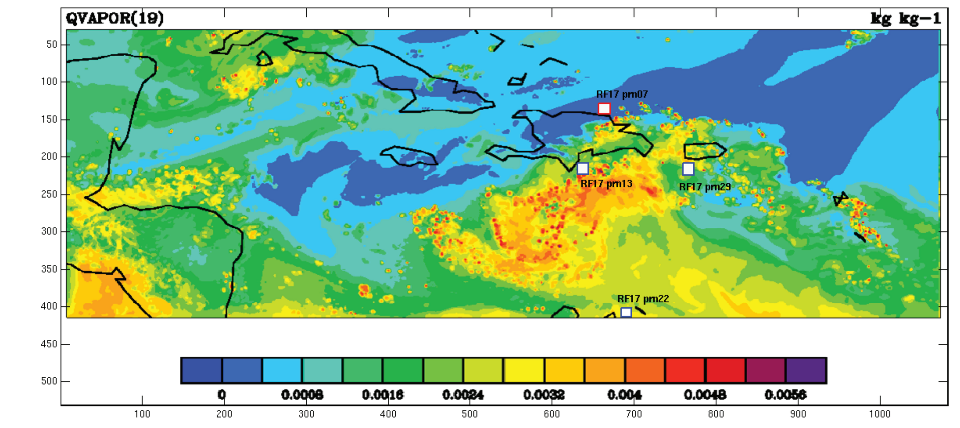

High-resolution water vapor fields from the DRPS (dropsonde only) data assimilation experiment at 12 Sept 1200 UTC at 6 km height. Locations of the occultation points for PRN07, PRN 13, PRN22, and PRN 29 are shown. PRN13 is located in a region of very high moisture, and PRN07 occurs in a very dry region.

COMPARISON WITH RADIO OCCULTATION DATA

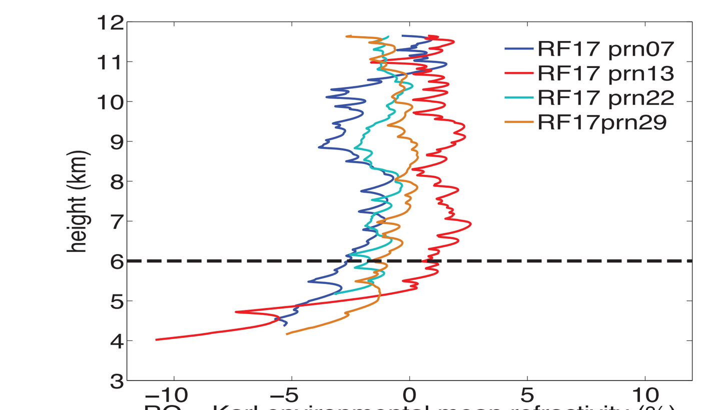

Retrieved refractivity minus the environmental mean at the location of the four occultations shown above. The environmental mean is calculated as the mean of all dropsondes in the 5 day period leading up to genesis. At 6 km height, PRN13 is has much higher refractivity, thus consistent with the profile occurring in a very moist region of the storm. This comparison illustrates that the implicit weighting of the observations to the location of the tangent point is sufficient to differentiate regions of vastly different moisture content, at the scale of ~250 km.

DROPSONDE + ARO ASSIMILATION RESULTS

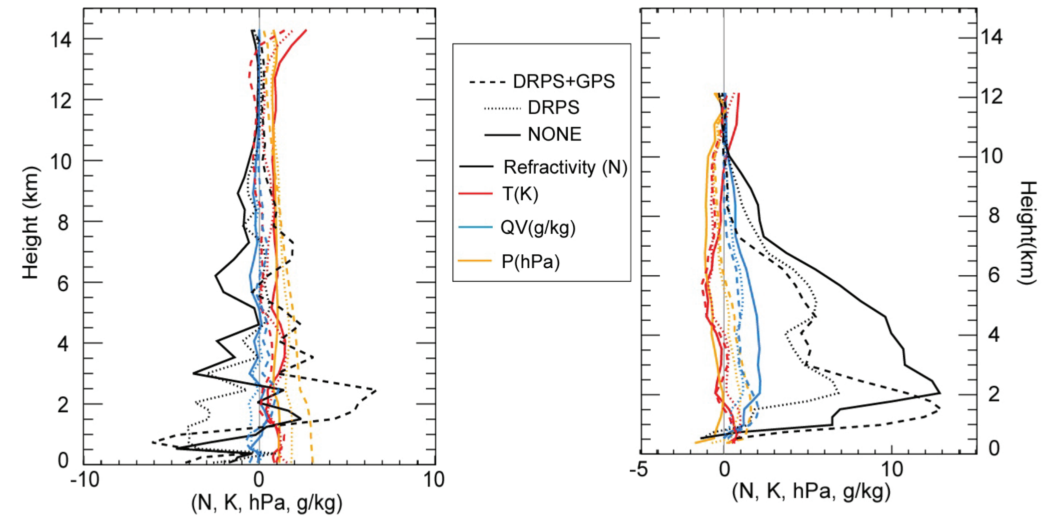

13 Sept 15:00 UTC *14 Sept 00:00 UTC*

Average difference in the refractivity, temperature, air pressure and water vapor mixing ratio between dropsonde observations and the WRF forecast simulation values at 13 Sept 15:00 UTC and 14 Sept 00:00 UTC (3 hours and 12 hours after the end of data cycling, respectively). Differences are small and perhaps insignificant after 3 hours. After 12 hours, however, the dropsondes improved the moisture fields substantially. Addition of the airborne GPS RO observations further improved the model moisture and refractivity fields above 4 km. Although there were no airborne observations at low levels, the simulations were indirectly affected by the observations assimilated in the levels above through the normal mode solution used in the vertical. Future improvements in ARO data analysis and retrieval methods are focused on altitudes below 4 km where atmospheric multipath can occur. This should help resolve the uncertainties in the model simulations near the surface.

CONCLUSIONS

Airborne GPS radio occultation refractivity profiles agree within ~ 2% of the refractivity calculated from nearby dropsondes and the ECMWF Interim Reanalysis, despite the small scale structures dominating the tropical cyclone environment. The bias is less than 1% above 6.5 km. This is the first demonstration of the close agreement between this new type of remote sensing data and conventional data.

In the 4 days leading up to genesis of the pre-Karl tropical storm, *GPS ARO profiles are consistent with the general increase in humidity in the vicinity of the storm center* measured by dropsondes. With more data we hope to quantify the distribution of moisture at different stages of development, which is critical to understanding the development of this storm.

Preliminary data assimilation using a non-local observation operator shows *forecast improvement for the dropsonde assimilation and the dropsonde + ARO assimilation tests above 4 km.*

Analysis of the 10 MHz high sample rate digitized GPS RF signals using *an open loop tracking algorithm extended the profile 2 km lower, demonstrating the ability of this technique to penetrate deeper into the moist atmosphere*. Using this technique, we will be able to recover many more profiles and achieve much denser sampling of the environment for each mission. This will also improve the statistical analysis of the results below 6.5 km as well as the assimilation results below 4 km.